BROOKHAVEN
NATIONAL LABORATORY

BNL-107370-2015-CP

9-D polarized proton transport in the MEIC "figure 8" collider ring – first steps

F. Meot[1], V. S. Morozov[2]

[1]Brookhaven National Laboratory, Upton, NY 11973 USA
[2]Jefferson Lab, Newport News, VA 23606 USA

Presented at the 6th International Particle Accelerator Conference (IPAC'15)
Greater Richmond Convention Center, Richmond, VA 23219 USA
May 3 – 8, 2015

May 2015

Collider Accelerator Department

Brookhaven National Laboratory

U.S. Department of Energy
Office of Science, Office of Nuclear Physics

DISCLAIMER

9-D POLARIZED PROTON TRANSPORT IN THE MEIC "FIGURE-8" COLLIDER RING - FIRST STEPS*

F. Méot, Collider-Accelerator Department, BNL, Upton, NY 11973
V.S. Morozov, JLab, Newport News, VA 23606

Abstract

Spin tracking studies in the MEIC figure-8 collider ion ring are presented, based on a very preliminary design of the lattice. They provide numerical illustrations of some of the aspects of the figure-8 concept, including spin-rotator based spin control, and lay out the path towards a complete spin tracking simulation of a figure-8 ring.

INTRODUCTION

Figure 1 and Table 1 summarize the characteristics and nominal parameters of the figure-8 ring, the optical functions are shown in Fig. 2 and Fig. 3. Details can be found in [1].

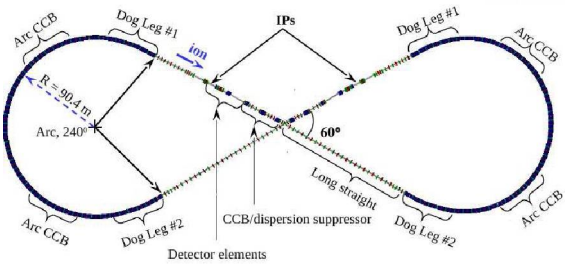

Figure 1: MEIC collider ion ring.

Table 1: Parameters of the 60 GeV MEIC figure 8 collider proton ring.

circumference	m	1415.3
energy	GeV	60
polarization goal	%	>70
H/V emittances	$\pi\mu$m	0.35 / 0.07
H/V β^*	cm	10 / 2
max. β_x / β_y	m	2301 / 2450
H/V tunes		25.79 / 26.27
H/V chromas, natural		-224 / -233
momentum compaction	10^{-3}	5.76
transition γ		13.18

* Work supported by Brookhaven Science Associates, LLC under Contract No. DE-AC02-98CH10886 with the U.S. Department of Energy. Authored in part by Jefferson Science Associates, LLC under U.S. DOE Contract No. DE-AC05-06OR23177 and DE-AC02-06CH11357. U.S. Government retains a license to publish or reproduce this manuscript for U.S. Government purposes.

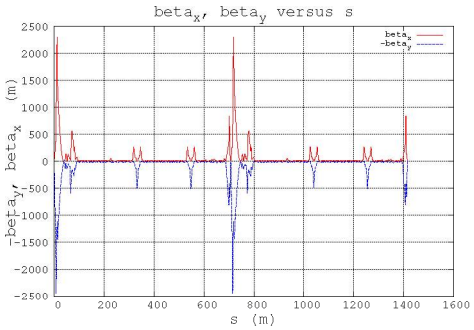

Figure 2: Betatron functions, horizontal and vertical.

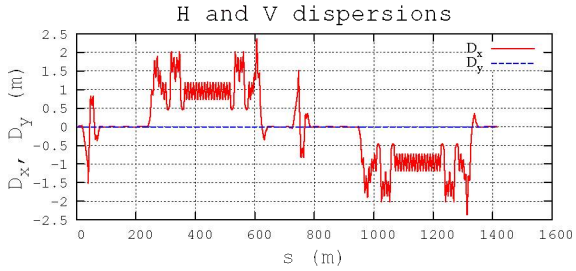

Figure 3: Dispersion functions, horizontal and vertical.

SPIN TRACKING

The present studies were done using a very preliminary design of the lattice, however not optimized for the spin dynamics and in particular not including the system intended for polarization control in MEIC. They can be viewed as simplified numerical illustrations of some of the aspects of the figure-8 concept, while laying out the path towards a complete spin tracking simulation.

Particle with zero initial coordinates

We start by tracking three particles with zero initial coordinates and with, respectively, fully longitudinal ($S_x^i = 1$), radial ($S_y^i = 1$), vertical ($S_z^i = 1$), initial spin orientation, for 200,000 turns through an ideal lattice containing no imperfections.

Figure 4-left shows the non-zero spin components of the three particles every 100 turns versus the turn number : the longitudinal spin component S_x of an initial $S_x^i = 1$ particle, the radial spin component S_y of a $S_y^i = 1$ particle, and the vertical spin component S_z of a $S_z^i = 1$ particle, all feature the same quasi-constant, quasi-unitary value vs. the turn number, as expected in a figure-8 ring. This validates the applicability of Zgoubi to this kind of study and demonstrates that it has the necessary numerical precision at least at the level of the chosen number of turns.

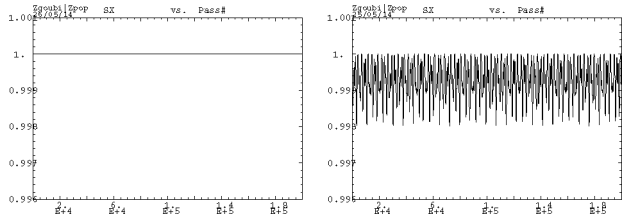

Figure 4: Left plot : case of a particle moving along the reference orbit in an ideal ring. Right plot : case of a particle launched with initial horizontal and vertical angles 0.2 mrad (i.e., with about *rms* H and V invariant values).

Effect of the betatron oscillations on spin

We next launch three particles from one of the MEIC interaction points (IPs), with all three different initial spin orientations as earlier, and with initial horizontal and vertical angles both of 0.2 mrad, which corresponds approximately to rms horizontal and vertical angular spreads. The particles are tracked for 200,000 turns, Fig. 5. Figure 4-right indicates that, for this order of the number of turns and still without lattice errors, there is no significant effect of the betatron oscillations on the spin motion in the figure 8 ring.

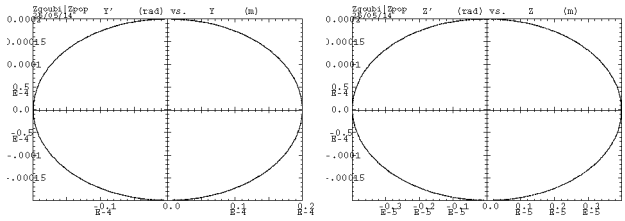

Figure 5: Horizontal (left) and vertical (right) 200,000 turn phase-space, for the particle launched with initial horizontal and vertical angles both 0.2 mrad in an ideal ring.

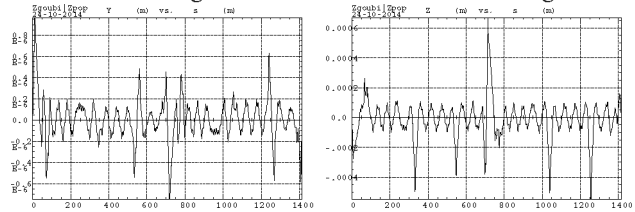

Figure 6: Closed orbits, horizontal and vertical, in the presence of a 0.2 mrad roll angle in an arc dipole.

Figure 5 shows the horizontal and vertical phase-space trajectories. The trajectories are consistent with the linear optics parameters at the observation point, the IP (the origin of the horizontal *s*-axis in Fig. 2). Note that there is no smearing of the trajectories, which is an indication that there is no symplecticity violation in Zgoubi, at least, at this level of the number of turns.

Misalignment effects

The spin motion in a figure-8 ring by itself is not stable because of the zero-harmonic imperfection spin resonance. The main contributions to the strength of this resonance come from the dipole roll and vertical quadrupole alignment errors [4]. Therefore, below we simulate the effects of these two types of errors and their compensation.

Dipole roll error Suppose that longitudinal beam polarization is required at the IP, which happens to be the particle launch location in our simulations. We introduce an imperfection in the lattice by rolling one of the arc dipoles by 0.2 mrad. Note that we do not then correct the closed orbit (essentially vertical, see Fig. 6). We track a particle with initially longitudinal spin direction for 200,000 turns. The particle is launched along the reference orbit. Note, however, that it still undergoes betatron oscillations due to the closed orbit distortion. The evolution of the particle's longitudinal spin component is plotted versus the turn number every 100 turns in Fig. 7.

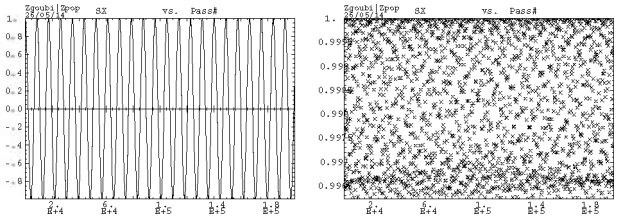

Figure 7: Longitudinal spin component S_x of the particle with initial $S_x^i = 1$. The particle is initially launched along the reference orbit in a ring with one of the arc dipoles rolled by 0.2 mrad. In the right plot case, the ring contains a spin rotator placed at the launch point, which rotates the spin by 1° about the longitudinal axis.

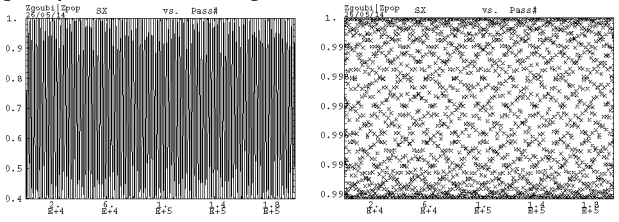

Figure 8: Longitudinal spin component S_x of the particle with $S_x^i = 1$. The particle is initially launched along the reference orbit in a ring with one of the arc quadrupoles misaligned vertically by 10 μm. In the right plot case, the ring contains a spin rotator placed at the launch point, which rotates the spin by 2° about the longitudinal axis.

Clearly, the longitudinal polarization direction is not preserved at the IP in Fig. 7-left. To correct for this effect of the dipole roll error, we install a zero-length spin rotator at the start of the lattice, which rotates the spin by 1° about the longitudinal axis but does not affect the orbital motion. Note that such a spin rotator can be installed anywhere in the experimental straight where the polarization is longitudinal. The dynamics of the longitudinal spin component in

the presence of the spin rotator is presented in Fig. 7-right.

Vertical quadrupole alignment error We next do a similar study of the effect of the vertical quadrupole alignment error. We misalign one of the arc quadrupoles vertically by 10 μm. We then track a particle with initially longitudinal spin direction launched along the reference orbit for 200,000 turns. The resulting behavior of the longitudinal spin component as a function of the turn number is shown in Fig. 8-left.

The longitudinal spin direction is again not preserved in Fig. 8-left. Similarly to the dipole roll case, we restore the longitudinal polarization direction by inserting a spin rotator at the beginning of the lattice, which rotates the spin by 2° about the longitudinal axis leaving the orbital motion unaffected. Note that a greater spin rotation angle is used in this case to attain better polarization preservation. This is not a general property of this kind of error but depends on the parameters of the ring, which have not been optimized in this version of the lattice for the spin dynamics in any way. The spin motion with the spin rotator is shown in Fig. 8-right.

Spin dynamics during acceleration

We insert a single zero-length RF cavity with parameters chosen such that it accelerates a proton beam from $G\gamma = 114.5$ ($p = 59.9153$ GeV/c) to $G\gamma = 115.5$ ($p = 60.4387$ GeV/c) in 200,000 turns with a synchronous phase of 20°. We first accelerate a particle with initially longitudinal spin on the reference orbit. Since the figure-8 ring is ideal and the numerical accuracy is adequate, the spin remains longitudinal throughout the acceleration process, Fig. 9.

We next simulated acceleration of a particle with the same 0.2 mrad dipole roll error as discussed earlier. The particle with initially longitudinal spin is launched along the reference orbit. As in the earlier study, there is no closed orbit correction. The resulting longitudinal spin component is plotted versus $G\gamma$ every 100 turns in Fig. 10-left.

To preserve the longitudinal polarization during acceleration, we insert a spin rotator as in the earlier studies, which rotates the spin by 5° about the longitudinal axis. To better understand the spin behavior, we accelerate at the same rate as before for 400,000 turns thus covering twice the energy range, from $G\gamma$ of 114.5 to 116.5. The longitudinal spin component as a function of $G\gamma$ is shown every 200 turns in Fig. 10-right. The nature of this behavior needs further study and understanding but the dips in the graph probably correspond to the points in energy of stronger zero-harmonic spin resonance strength. Finally, Fig. 11 plots $G\gamma$ and kinetic energy, respectively, from the same simulation as functions of the turn number every 200 turns to confirm that acceleration was simulated correctly.

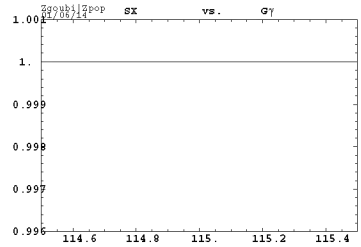

Figure 9: Longitudinal spin component S_x of the particle with initial $S_x^i = 1$, vs. $G\gamma$. The particle accelerates along the reference orbit in an ideal ring.

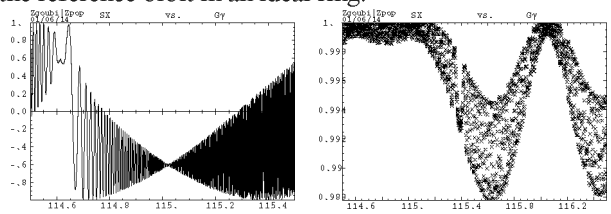

Figure 10: Longitudinal spin component S_x of a particle with $S_x^i = 1$, vs. $G\gamma$, over 200,000 turns (left) and 400,000 turns (right). The particle is initially launched along the reference orbit in a ring with one of the arc dipoles rolled by 0.2 mrad. In the right plot case, the ring contains a spin rotator placed at the launch point, which rotates the spin by 5° about the longitudinal axis.

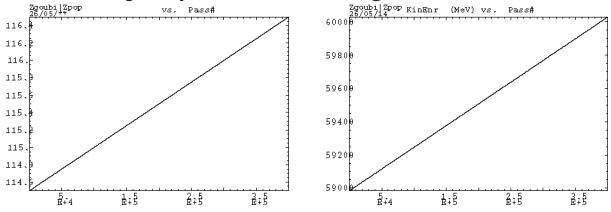

Figure 11: $G\gamma$ (left) and kinetic energy (right) plotted vs. the turn number every 200 turns, over 400,000 turns. The particle is initially launched along the reference orbit in a ring with one of the arc dipoles rolled by 0.2 mrad.

REFERENCES

[1] F. Lin, *MEIC Project at Jefferson Lab*, EIC14 workshop, March 17-21, 2014, Thomas Jefferson National Accelerator Facility, Newport News, VA. http://appora.fnal.gov/pls/eic14/agenda.full.

[2] F. Méot, Zgoubi Users' Guide, Report C-A/AP/470, BNL C-AD, October 2012.

[3] Zgoubi and its guide, examples, zpop post-processor, toolbox, are available at http://sourceforge.net/p/zgoubi/code/HEAD/tree/. The toolbox provides various software such as a translator from MADX (or MAD8), closed orbit search, dynamic aperture search, spin $\vec{n}_0$ search, spin distribution or spin tune computation, and a lot more.

[4] Ya.S. Derbenev *et al.*, *"Ion polarization control in MEIC rings using small magnetic field integrals"*, in Proc. of PSTP 2013, Charlottesville, VA).